

## FEDSM-ICNMM2010-1000

### DIFFUSIONAL MASS TRANSFER AT THE SURFACE OF SMALL GAS BUBBLES

**Jan-Peter Jeskulke**

Fluid Mechanics  
Department of Mechanical Engineering  
University of Bochum  
Bochum, Germany

**Franz Peters\***

Fluid Mechanics  
Department of Mechanical Engineering  
University of Bochum  
Bochum, Germany  
Email: franz.peters@rub.de

#### ABSTRACT

*A method apt to observe small levitated bubbles in the sub-mm range in liquid is described. The method combines a rotary chamber with a Mie scattering method. The key result of the measurements with this method is the rate at which gas diffuses from the bubble into the liquid. A remarkable result is found for five different gases in water. It turns out that the mass flux density is independent of the radius. This suggests that convective mass transport is not the controlling mechanism.*

#### NOMENCLATURE

D diffusion coefficient [ $m^2/s$ ]  
 $\dot{m}$  mass flux [ $kg/s$ ]  
 $\Omega$  angular velocity [ $s^{-1}$ ]  
R bubble radius [ $m$ ]  
 $\rho$  density [ $kg/m^3$ ]  
t time [ $s$ ]  
y coordinate [ $m$ ]

#### INTRODUCTION

Gases have a solubility in liquids that depends on pressure and temperature. Whenever the equilibrium between gas and liquid is unbalanced diffusion takes place aiming to re-establish equilibrium. The rate at which diffusion takes place is a key issue in chemical engineering processes. Of particular interest are small bubbles with their large surface to volume ratio. Due to buoyancy they induce automatically a steady upwards rise with a corresponding flow field.

Diffusion models on bubbles do exist [1] yet there is no experimental confirmation. One reason is that the flow past the bubble is not well known due to the complicated problem of mobile and immobile surfaces [2]. The other reason is that studies on small bubbles in the sub-mm range are difficult because the rising bubble provides only a transient image to the observer. We have introduced a rotary chamber method [3] by which the bubble can be locally levitated in a downward flow. There it can be observed for as long as it exists. Depending on the initial degree of saturation the bubble either maintains its size or shrinks by diffusion. The rate at which this happens is accurately measured by a Mie-scattering method. Microscopic imaging techniques would also be possible, yet this method seems superior when very small bubbles are considered.

We have studied how air, nitrogen, butane, helium and argon diffuse into water. The initial bubble radii were in the 500 – 600  $\mu m$  range. The bubbles could be observed down to 100  $\mu m$ . The paper presents the method together with a first set of data.

---

\*Address all correspondence to this author.

## EXPERIMENTAL

The experiment combines the rotating chamber with a Mie scattering optical set-up. The rotating chamber provides a bubble levitated in a downward flow while the optical set-up allows the precise evaluation of the bubble size versus time as long as the bubble is spherical.

### The rotating chamber

The study of droplets levitated in a gas by e.g. acoustical waves is well established [4] while the inverse problem of bubble levitation in liquids remains difficult. We have made substantial progress with the rotating chamber [3]. As sketched in Fig. 1 a volume of liquid is enclosed between two parallel glass plates of optical quality ( $\lambda/10$ ). The plates are separated by a spacer from plastic material and framed by aluminium rings. These rings run on two cylindrical rolls which are driven by a frequency controlled motor. This way the chamber rotates about its axis together with the enclosed liquid at a known angular frequency  $\Omega$ .

A small bubble injected into the liquid by a syringe propagates to a final destination close to the horizontal where it becomes levitated. The fact that levitation is attained means a vertical as well as a horizontal balance of forces. In vertical direction the downward drag force equilibrates the buoyancy. In horizontal direction the lift force which comes about through the curved streamlines balances the rotational pressure gradient. For a given angular velocity the initial position of the bubble depends on its radius. When the bubble is started at an outer radius it shrinks by diffusion of bubble gas into the surroundings and consequently moves slowly inwards.

In order to observe the travelling bubble it becomes necessary to either move the chamber or the observer. In the present set-up the observer is fixed and the chamber with its support moves controlled by a precise x-y positioning system. By monitoring the displacement the radial position of the bubble with respect to the axis of rotation is always known.

Obviously the rate of diffusion depends on the degree of gas saturation of the liquid. For a full treatment of the problem this would be needed. Unfortunately, there is no instantaneous probe measurement to make it readily available. Therefore, for the time being we had to resort to the case of a degassed liquid. Degassing was achieved by applying a vacuum pump to the gas volume on top of the liquid until the vapour pressure of water was established. To provide sufficient degassing nuclei some activation with a magnetic stirrer is advisable.

The temperature in all experiments was  $20 \pm 0.5^\circ\text{C}$ .

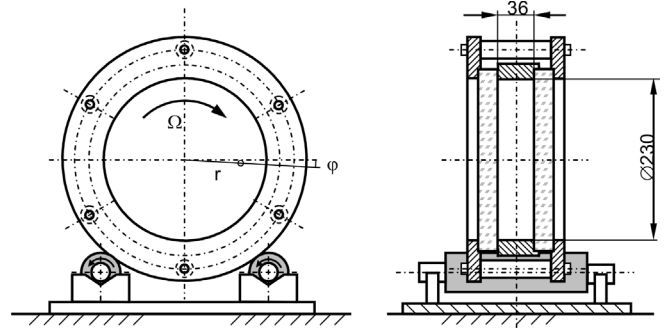


FIGURE 1. ROTARY CHAMBER WITH LEVITATED BUBBLE

### Optical set-up and analysis

Mie scattering was analytically treated by Mie already in 1908 [5]. It became available for measuring purposes with the advent of the laser and the computer, because it requires monochromatic coherent light and extensive calculations of the Mie functions. Mie codes are preferably written following the book by Bohren et al. [6]. A number of codes are available in the internet. Mie scattering theory predicts how light is scattered by a spherical transparent object when placed into a laser beam.

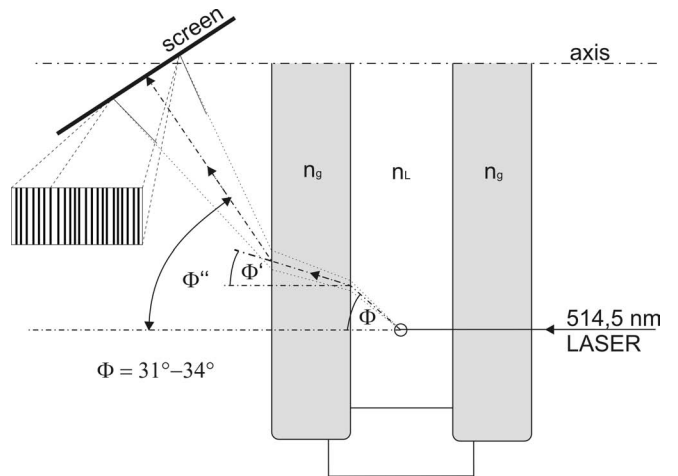


FIGURE 2. HORIZONTAL CROSS-SECTIONAL VIEW THROUGH ROTARY CHAMBER WITH COURSE OF RAYS.

On a screen held at a distance from the sphere the scattered light forms interference fringes. The interference takes place among elementary waves originating from the sphere at different phases. The fringe pattern depends on the wavelength, the observation direction relative to the laser, the laser polarization, the refractive indices and the radius of the sphere. When

everything else is known the radius can be evaluated from the fringe pattern.

Our principle optical set-up is shown in Fig. 2. An Argon-Laser operated at  $514,7nm$  and polarized normal to the paper plane illuminates the bubble. With  $2mm$  the laser beam is larger in diameter than the bubble. The scattered light undergoes two deflections when passing the glass wall. This has to be accounted for when a scattering angle is assigned to the fringe location on the screen. The fringes are parallel to the direction of polarization.

Not shown is the 8-bit CCD-camera (256 gray values) by which the fringe pattern is photographed. The fringe evaluation for the bubble radius comprises three steps.

- the image of the fringe pattern has to be post-processed.
- the fringe pattern has to be calculated from Mie theory for a suitable spectrum of radii.
- by comparison of experimental and calculated patterns that particular radius has to be identified that provides best agreement.

From preliminary work on various scattering angles it turned out that the range from  $31^\circ$  to  $34^\circ$  would be a fair choice. Therefore all images were exactly tailored to this range. The post-processing of the raw image included the following steps:

- Gauss filtering smoothens local disturbances
- In fringe direction the images were limited to a fraction of the lateral extension. The statistical fluctuation of the gray value in fringe direction was eliminated by taking the average.
- The resulting gray values are normalized to the 8-bit resolution.

Figure 3 shows a result. The enhanced fringe pattern between  $31^\circ$  and  $34^\circ$  is seen on top. The corresponding gray value profiles are plotted below. The larger signal is normalized to the 8-bit scale.

The theoretical gray value profile is calculated from Mie theory. For comparison of experimental and theoretical profiles a direct overlay is feasible for a single case yet too cumbersome for series of cases. Therefore, Fast Fourier Transform (FFT) was employed with the objective to find the fringe frequency within the fixed angular interval.

First the theoretically calculated profiles for each radius were subjected to FFT. A typical answer is shown in Fig. 4. A unique frequency is found expressed as peaks/degree. The smaller side peaks are due to the fact that the frequency within the interval is (according to Mie theory) not exactly constant. Calculations up to almost  $2000\mu m$  in diameter produced the

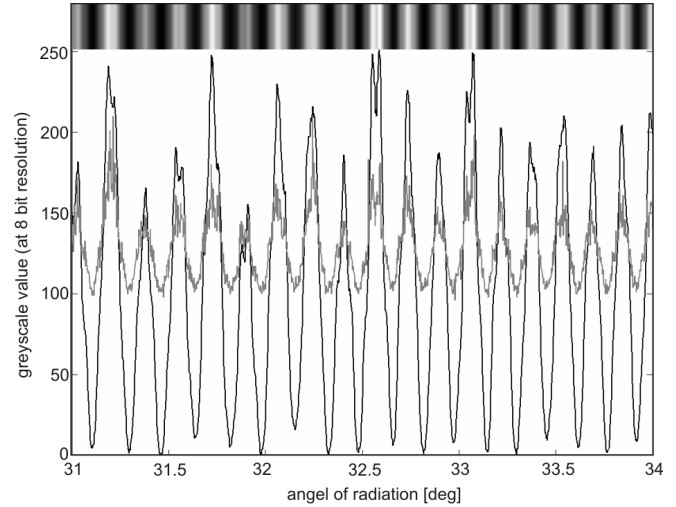


**FIGURE 3.** TOP: THE EXPERIMENTAL MIE SCATTERING FRINGE PATTERN. SMALL SIGNAL: THE ASSOCIATED GRAY VALUE PROFILE. LARGE SIGNAL: THE NORMALIZED GRAY VALUE PROFILE.

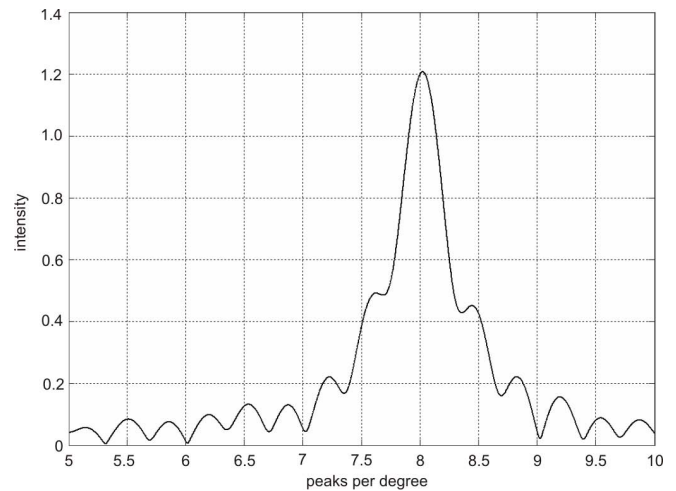


**FIGURE 4.** FFT-ANALYSIS OF THE GRAY VALUE PROFILE BETWEEN  $31^\circ - 34^\circ$  FOR A DIAMETER OF  $997\mu m$

perfectly linear relationship of Fig. 5. With respect to our purpose this figure reduces the content of the Mie theory to a single curve for the selected angular interval. The remaining step to be done is to run the FFT over the experimental signal in the same interval, get the frequency and read the diameter from Fig. 5.

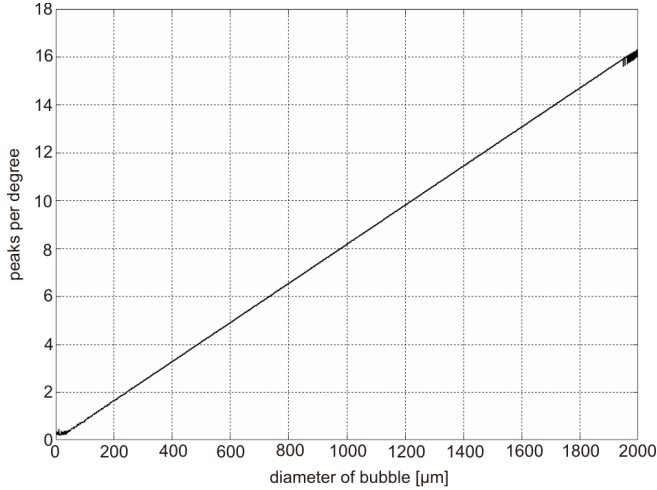


FIGURE 5. THE PEAK FREQUENCY VERSUS DIAMETER

## RESULTS AND DISCUSSION

By taking a time sequence of bubble fringe patterns as the bubble moves radially inwards and running these patterns through the evaluation procedure as explained the bubble radius as function of time  $R(t)$  becomes available. With the rotational velocity of the chamber and the radial position of the bubble the rise velocity as function of radius can immediately be extracted. The results are displayed in Fig. 6.

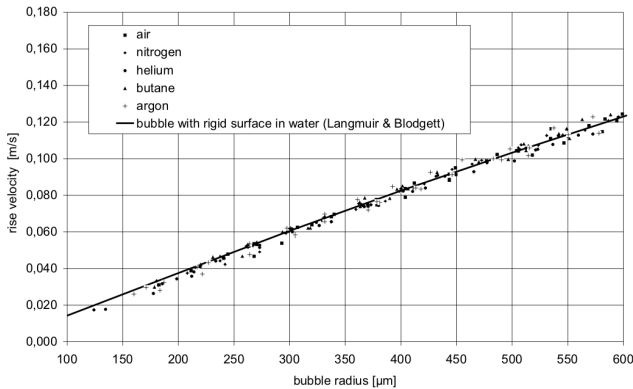


FIGURE 6. RISE VELOCITY OF BUBBLES IN WATER

All bubbles for five different gases follow a common line which is the rise velocity of solid spheres. This surprising behaviour is well known (Clift [7]). It is attributed to the presence of an immobile surface which is due to surface active traces of surfactants.

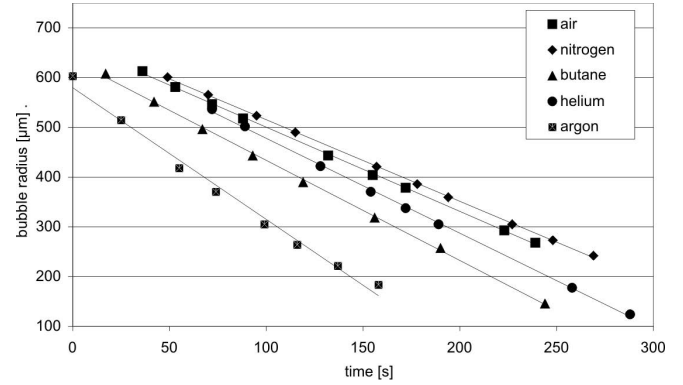


FIGURE 7. BUBBLE RADIUS VERSUS TIME FOR DIFFERENT GASES IN WATER

The derivative of the radius with respect to time is called the diffusion velocity. The product of the diffusion velocity with the bubble area and the density of the gas yields the mass flux of gas being transferred to the liquid

$$\dot{m} = \rho_G 4\pi R^2 \frac{dR}{dt}. \quad (1)$$

In order to assess the intensity of the mass transfer the mass flux per unit area is more significant which is at the same time the diffusion velocity times the gas density.

Figure 7 shows the radius vs. time traces for five different gases in degassed and de-ionized water. The covered radius ranges from  $600$  to  $100\mu m$ . The total observation time stays below 5 minutes. The slopes of these curves, i.e. the diffusion velocities are plotted in Tab. 1 together with the mass flux and other parameters.

The bubble radius determines the rising velocity (Fig. 6). The Reynoldsnumber grows with radius as the velocity grows with it. A changing Reynoldsnumber entails a changing flow field. A changing flow field, again, is expected to affect the mass transfer. Therefore, it is a striking feature that the diffusion velocities do not depend on the radius. It seems that the mass transfer process concentrates at the interface in a very thin layer where convective transport at the existing low Reynoldsnumbers becomes negligible. Therefore, the controlling mechanisms are most likely adsorption and diffusion right at the interface. Under the assumption that adsorption is fast enough to saturate the adjacent liquid at all times the highest possible concentration (solubility) and the diffusion coefficient are the key parameters. The concentration difference between saturated interface and the degassed surroundings will be the driving potential. Tab. 1 refers to literature values of diffusion coefficient and solubility.

**TABLE 1.** RESULTS FOR FIVE GASES IN DE-IONIZED WATER AT 20°C. DATA FROM [8]

	$dR/dt$ [ $\mu\text{m}/\text{s}$ ]	mass flux [ $\text{kg}/\text{m}^2\text{s}$ ]	diffusion coefficient [ $\text{m}^2/\text{s}$ ]	solubility [ $\text{kg}/\text{m}^3$ ]	conc. at the interface [ $\text{kg}(\text{gas})/\text{m}^3(\text{w.})/\text{m}$ ]	gradient
Argon	2.65	$4.34 \cdot 10^{-6}$	$2.0 \cdot 10^{-9}$	$5.46 \cdot 10^{-2}$	36811	
Butane	2.01	$4.81 \cdot 10^{-6}$	$0.96 \cdot 10^{-9}$	$6.09 \cdot 10^{-2}$	81879	
Helium	1.91	$0.31 \cdot 10^{-6}$	$5.8 \cdot 10^{-9}$	$0.15 \cdot 10^{-2}$	37310	
Air	1.69	$2.00 \cdot 10^{-6}$	$2.3 \cdot 10^{-9}$	$2.14 \cdot 10^{-2}$	42374	
Nitrogen	1.64	$1.89 \cdot 10^{-6}$	$2.1 \cdot 10^{-9}$	$1.73 \cdot 10^{-2}$	54427	

Argon shows the highest diffusion velocity. This makes sense because argon has the highest solubility in combination with a medium diffusion coefficient. Helium is known for very high diffusivity (being used for leak detection). Yet, in combination with a low solubility it lacks driving potential and the resulting diffusion velocity is even smaller than that of butane which represents a relatively huge molecule ( $C_4H_{10}$ ). Air and nitrogen are not much different as can be expected.

A parameter that can be extracted is the concentration gradient at the interface listed in Tab. 1. It simply follows from Fick's law when convection is neglected

$$\dot{m} = -4\pi R^2 D \left. \frac{d\rho}{dy} \right|_{y=0}. \quad (2)$$

Here  $\rho$  is the density and  $\dot{m}$  the mass flux that we have determined. When this gradient is linearly extrapolated to the zero concentration in the surroundings we get an order of magnitude of the thickness of the diffusion layer. It turns out to be very thin with  $1\mu\text{m}$  for argon.

## SUMMARY

We have presented an experimental method apt to measure the rate at which small levitated bubbles give off gas to the surrounding liquid. The experiment is based on a rotating chamber providing levitation and on Mie light scattering serving as a size measuring tool.

Five different gases were investigated in degassed and de-ionized water at 20°C. The size range was 600 to  $100\mu\text{m}$  in radius. The most important result is the following. The diffusion velocity comes out constant for all gases. It means that the mass flux density is constant while the bubble radius changes. It may be followed that the flow field with its convective properties has

little influence on the mass transfer. The diffusion in turn takes place in a very thin layer of the order of  $\mu\text{ms}$ .

From the results the diffusion coefficient cannot readily be obtained because we have no means to detect the concentration gradient at the interface. On the other hand the experiment provides directly what rising bubbles do. This is important knowledge especially for bubble reactors and gassing of liquid pools.

The most important step in upgrading the method would be the development of an independent method for the determination of the actual gas concentration before the diffusion velocity is measured.

## ACKNOWLEDGMENT

This work was supported by the Deutsche Forschungsgemeinschaft DFG (Pe 401/27-1).

## REFERENCES

- [1] Mersmann, A., 1986. *Stoffübertragung*. Wärme- und Stoffübertragung. Springer, Berlin.
- [2] Lakshmanan, P., and Ehrhard, P., 2010. "Marangoni effects caused by contaminants adsorbed on bubble surfaces". *Journal of Fluid Mechanics*, **647**(1), pp. 143–161.
- [3] Peters, F., and Biermann, S., 2004. *Streulichtuntersuchungen an einem kleinen, levitierten Bläschen: Lasermethoden in der Strömungsmesstechnik: Tagungsband zur 12. Fachtagung*. GALA e.V., Karlsruhe.
- [4] Davis, E. J., and Schweiger, G., 2002. *The airborne microparticle: Its physics, chemistry, optics, and transport phenomena*. Springer, Berlin.
- [5] Gustav Mie, 1908. "Beiträge zur Optik trüber Medien, speziell kolloidaler Metallösungen". *Annalen der Physik*, **330**(3), pp. 377–445.
- [6] Bohren, C. F., and Huffman, D. R., 2004. *Absorption and*

*scattering of light by small particles*, [repr.] ed. Wiley-VCH, Weinheim.

- [7] Clift, R., Grace, J. R., and Weber, M. E., 2005. *Bubbles, drops, and particles*. Dover Publ., Mineola, N.Y.
- [8] Andrussov, L., Schramm, B., and Schäfer, K., 1969. *Viskosität und Diffusion*, sechste Aufl. ed., Vol. A ED.6 of *Zahlenwerte und Funktionen aus Physik, Chemie, Astronomie, Geophysik und Technik / Landolt-Börnstein*. Springer, Berlin etc.